

Ultrasound imaging features of bronchial anthracofibrosis

xiaofeng lu

People's Hospital of Honghuagang District

daishun liu

Zunyi Medical College Affiliated Hospital: Affiliated Hospital of Zunyi Medical University

xiaoyan cai

People's Hospital of Honghuagang District

qingshong zeng

Batibo District Hospital

li zou

People's Hospital of Honghuagang District

zuoli du

People's Hospital of Honghuagang District

guoqi zhou (✉ 916071126@qq.com)

hospital <https://orcid.org/0000-0002-6477-668X>

Research article

Keywords: Anthracosis, Ultrasound imaging, Chronic obstructive pulmonary disease, Bronchoscopy, Biofuel, Airway remodeling, Pneumoconiosis

Posted Date: July 23rd, 2021

DOI: <https://doi.org/10.21203/rs.3.rs-738220/v1>

License:  This work is licensed under a Creative Commons Attribution 4.0 International License.

[Read Full License](#)

Abstract

Purpose

To determine the ultrasound imaging characteristics of participants with bronchial anthracofibrosis (BAF) and identify clinical markers for prevention and treatment.

Methods

We randomly selected 1,243 participants (including 113 with BAF) who underwent bronchoscopy and treatment at our institution from April 2018 to October 2019. BAF was classified as flat, deep seated retracted, or mucosal protrusion type, based on microscopy. Ultrasound probes were used to determine the maximum thickness of the tube wall and submucosa. The average values of the submucosal and bony tissue areas of the BAF subtypes were compared.

Results

The BAF group included 13 participants with a history of tuberculosis (11.5%) and 57 with biofuel exposure (50.4%). The average exposure time was 17.4 ± 6.2 years; BAF accounted for 10% of bronchoscopies performed. The maximum tube-wall thicknesses of the deep-seated retracted (17.3 ± 5.7) and black protruding (19.3 ± 5.4) groups were significantly greater than that of the flat group (12.5 ± 5.0 ; $P < 0.05$). The maximum thicknesses of the submucosa in the deep-retracted (9.8 ± 3.0) and black protruding (14.5 ± 5.0) groups were significantly greater than that of the flat group (6.6 ± 3.5 ; $P < 0.05$). The ratios of bone tissue in the flat and black protruding groups were $33.3 \pm 9.3\%$ and $34.9 \pm 12.1\%$, respectively; the ratio in the deep-seated retracted group ($65.2 \pm 8.7\%$) was significantly reduced ($P < 0.05$). The flat type showed no significant change ($P > 0.05$).

Conclusion

Differences in BAF airway remodeling among the different subtypes may lead to varying clinical symptoms. Analyzing the characteristics of BAF airway remodeling and the regulatory pathway may provide new clues for treatment.

Introduction

Bronchial anthracofibrosis (BAF) is a pulmonary disease caused by the accumulation of carbon in the lungs due to repeated exposure to air pollution or inhalation of smoke or coal dust particles[1]. The prevalence of BAF in the general population can only be roughly estimated, as diagnosis requires bronchoscopy. Large studies of participants who underwent bronchoscopy for other reasons have shown the prevalence of simple anthracosis to be 3.4–21%[2]. As auxiliary examinations other than

bronchoscopy lack specificity, it is difficult to distinguish BAF from pulmonary tuberculosis (TB), chronic obstructive pulmonary disease, and malignant neoplasms through routine examinations such as pulmonary function tests and computed tomography[3]. A thorough understanding of the clinical characteristics of BAF may facilitate the acquisition of epidemiological data. At present, extensive investigations of the endobronchial ultrasound (EBUS) imaging features of participants with BAF have not been reported. Mirsadraee and Farshchi[4] reported a case of typical anthracosis with a scattered nodular hyperechoic pattern in the subepithelial area of the bronchus or lymph node adjacent to the bronchial mucosa. However, in-depth research on this aspect is insufficient. Therefore, we analyzed the EBUS imaging features of participants with BAF to provide effective clinical clues for the prevention and treatment of the disease.

Materials And Methods

Participants

This study was approved by the ethics committee of the People's Hospital of Honghuagang District. Due to the retrospective nature of the study, the requirement for informed consent was waived. Among 1,243 participants who underwent bronchoscopy and treatment at the Department of Respiratory and Critical Care Medicine at the People's Hospital of Honghuagang District in Zunyi, China, between April 2018 and October 2019, 113 participants with a diagnosis of BAF were randomly selected for this study. BAF diagnoses were established in accordance with the criterion reported in the literature[5], that is, typical dark anthracotic pigmentation on the bronchial mucosa visible via electronic bronchoscopy.

The general demographic data of the study participants, such as age (years) and sex, were recorded. The following clinical data were also collected: history of TB, exposure or non-exposure to biofuels, duration of biofuel exposure (years), smoking history, body mass index (BMI), and history of comorbidities, such as diabetes, ischemic heart disease, stroke, chronic liver disease, chronic kidney disease, or hyperlipidemia.

Routine bronchoscopy

Bronchoscopy is the gold standard procedure performed to establish the diagnosis of anthracofibrosis. In the present study, an EB-530T electronic bronchoscope (Fujifilm, Japan) was used for examination and imaging of all participants (as far as possible, up to the segmental bronchi and trachea). In accordance with the criteria reported in the literature[6], the participants were classified as having flat BAF, deep-seated retracted BAF (originating from an anthracotic lymph node beside the bronchus), or black mucosal protruding BAF (with or without narrowing of the bronchi) based on bronchoscopic images. In addition to black lesions, other pathological changes (e.g., bronchial swelling or obliteration) visible under bronchoscopy, and their locations, were recorded.

EBUS

The EBUS system (PB2020-M) and supplies used in this study were purchased from Fujifilm (Japan). During each EBUS examination, a mini-probe (external diameter: 1.9 mm, acoustic frequency: 20 MHz) was inserted into the 2.8-mm forceps channel, and ultrasound images were obtained through the working channel of a video endoscope (SP-900). Examinations were performed using the 360° sweep B-scan ultrasound mode, and results were recorded on a computer.

Single-blind analysis of the EBUS images was performed using ImageJ (version 1.48c, NIH, USA). The measured and analyzed parameters included bronchial diameter (calculated by taking the average value of two vertical diameter measurements in each airway), internal perimeter, maximum bronchial wall thickness, and maximum submucosal thickness. For all airways, the average values of the diameter, internal perimeter, lumen area, submucosal area, and bony tissue area were calculated. The same observer analyzed 14 EBUS images thrice over intervals of ≥ 1 week to assess the repeatability of the measurements.

Statistical analyses

Data analysis was performed using the Statistical Package for the Social Sciences (version 23.0; International Business Machines Corp., Armonk, NY, USA). Continuous variables were expressed as the mean \pm standard deviation, and categorical variables were expressed as numbers and percentages. Comparisons of continuous variables between two groups were performed using the independent samples t-test, comparisons of continuous variables between multiple groups were performed using analysis of variance, pairwise comparisons of continuous variables were performed using the least significant difference test, comparisons of categorical variables between groups were performed using the χ^2 test, and pairwise comparisons of categorical variables were performed using the Bonferroni correction. Values of $P < 0.05$ were considered statistically significant.

Results

General data

A total of 113 participants with BAF with a mean age of 66.2 ± 9.3 years were included in the present study; 53 participants (46.9%) were men, the mean BMI was 21.6 ± 3.7 kg/m², and 42 participants (37.2%) were smokers. Thirteen participants (11.5%) had a history of TB, which may be associated with a high prevalence of TB in the region where this study was conducted, and 57 participants (50.4%) had been exposed to biofuels for a mean duration of 17.4 ± 6.2 years. The comorbidities of the participants were as follows: diabetes mellitus (4 participants, 3.5%), ischemic heart disease (22 participants, 19.4%), chronic liver disease (one participant, 0.14%), chronic kidney disease (one participant, 0.14%), and hyperlipidemia (26 participants, 23.0%).

Bronchoscopy results

Under bronchoscopy, participants with flat BAF (Figure 1A) exhibited an unobstructed lumen with normal morphology; absence of evident mucosal hyperemia, edema, and thickening; and a sharp-appearing bronchial carina. In participants with deep-seated retracted BAF (Figure 1B), we observed evident fibrous tissue proliferation, slight distortion of the lumen, stenosis of the affected bronchi (commonly occurring as external compression-type stenosis), slight hyperemia in the mucosa, and a sharp-appearing bronchial carina. Additionally, difficulties were encountered during the biopsy procedures of these participants. Bronchoscopy of participants with black mucosal protruding BAF (Figure 1C) revealed severe distortion of the lumen; evident lumen stenosis often accompanied by bronchial obliteration; evident mucosal hyperemia, edema, and thickening; a broadened and deformed bronchial carina with occasional mucosal ulceration or necrosis; and high bleeding tendency upon contact with the bronchoscope. Significant post-biopsy bleeding was observed (four participants experienced bleeding during bronchial brushing), and bleeding control was relatively difficult. However, effective control was achieved after subsequent treatment. Among the 113 participants with BAF, 31 (27.4%) had flat BAF, 38 (33.6%) had deep-seated retracted BAF, and 44 (38.9%) had black mucosal protruding BAF.

EBUS examination results

EBUS examinations using a mini-probe revealed the following manifestations in the airways of the healthy control and BAF groups: (1) the healthy control group (Figure 2A) showed uniform aeration patterns in the peripheral lung tissue, (2) the flat BAF group (Figure 2B) showed uniform aeration patterns in the lung tissue, (3) the deep-seated retracted BAF group (Figure 2C) showed disordered lung tissue signals with scattered calcification patterns, (4) and the black mucosal protruding BAF group (Figure 2D) showed soft tissue patterns in the lung tissue. Figure 3 shows the ImageJ 18.0-magnified ultrasound images and transbronchial lung biopsy specimens of an airway with BAF.

The magnified ultrasound images of the bronchial walls of participants in various groups revealed the following manifestations: (1) The healthy control group showed a regular circular distribution of the airway wall, occasional shadows on the cartilage rings, uniform mucosa, and uniformly dense submucosal tissue; (2) the flat BAF group showed a decreased mucosal area compared with the healthy control group and uneven thickening of submucosal tissue; (3) the deep-seated retracted BAF group showed a decreased mucosal area compared with the healthy control group, significant thickening of the cartilage layer, and uneven calcification on the airway wall; (4) and the black mucosal protruding BAF group showed a decreased mucosal area, uneven thickening of submucosal tissue, and a disorderly arrangement of cartilage tissue.

Table 1 shows the airway wall indicators of the various BAF subgroups measured after magnification of the ultrasound images using ImageJ 18.0. The maximum wall thicknesses of the flat BAF, deep-seated retracted BAF, and black mucosal protruding BAF groups were 12.5 ± 5.0 mm, 17.3 ± 5.7 mm, and 19.3 ± 5.4 mm, respectively, with multigroup comparisons showing statistically significant differences ($F=14.946$, $P=0.000$). Pairwise comparisons showed that the maximum wall thicknesses of the deep-seated retracted BAF and black mucosal protruding BAF groups were significantly higher compared with that of the flat

BAF group ($P<0.05$), but the difference in maximum wall thickness between the deep-seated retracted BAF and black mucosal protruding BAF groups was not statistically significant ($P=0.090$). The maximum submucosal thicknesses of the flat BAF, deep-seated retracted BAF, and black mucosal protruding BAF groups were 6.6 ± 3.5 mm, 9.8 ± 3.0 mm, and 14.5 ± 5.0 mm, respectively, with multigroup comparisons showing statistically significant differences ($F=36.819$, $P=0.000$). Pairwise comparisons showed that differences among the three groups were statistically significant ($P<0.05$). The proportions of bony tissue area in the flat BAF, deep-seated retracted BAF, and black mucosal protruding BAF groups were $33.3\pm 9.3\%$, $65.2\pm 8.7\%$, and $34.9\pm 12.1\%$, respectively, with multigroup comparisons showing statistically significant differences ($F=113.473$, $P=0.000$). Pairwise comparisons revealed that the bony tissue area of the deep-seated retracted BAF group was significantly higher compared with those of the other two groups ($P<0.05$), but the bony tissue area of the black mucosal protrusion BAF group did not differ significantly from that of the flat BAF group ($P=0.508$). The proportions of submucosal area in the flat BAF, deep-seated retracted BAF, and black mucosal protruding BAF groups were $64.8\pm 9.1\%$, $30.4\pm 8.8\%$, and $58.6\pm 11.7\%$, respectively, with multigroup comparisons showing statistically significant differences ($F=120.031$, $P=0.000$). Pairwise comparisons indicated that differences among the three groups were statistically significant ($P<0.05$).

Discussion

BAF was first described as black discoloration of the bronchial mucosa (simple anthracosis) or scattered foci of black spots that retract the mucosa inward due to the effect of adjacent anthracotic lymphadenopathy and cause changes in bronchial structures. Given the lower prevalence of BAF in Western countries, interest in this disease has gradually declined in the West. However, it is considered a common disease in Asia, as the literature has reported the occurrence of a second wave of anthracosis on the continent. Chung et al.[7] considered BAF a unique clinical syndrome that distorts and narrows the bronchial lumen in severe cases. Therefore, clinicians have introduced terms such as anthracostenosis[8] and anthracotic bronchitis[9] to describe the resultant changes in bronchial structure. In the majority of cases, BAF is accompanied by severe submucosal edema, bronchial stenosis, protruded mucosal folds, and lung collapse[9]. Due to the lack of conclusive epidemiological data and the fact that bronchoscopy is the gold standard procedure for anthracosis diagnosis, it is difficult to estimate the prevalence of BAF in the general population. The prevalence of BAF is lower in Western countries, with Wynn et al. reporting only seven BAF cases among 7,000 bronchoscopies[10]. Reports of BAF from other continents, such as North America and Africa, are also rare[11]. Available data from a large series of participants who underwent bronchoscopy for other reasons have shown the prevalence of BAF to be 3.4–21%[2]. Recently, researchers in China have begun to show a keen interest in the clinical presentations of BAF, but in-depth studies on Chinese populations remain scarce[12]. Through our retrospective analysis of data from participants who underwent bronchoscopy at our hospital, we determined a BAF prevalence rate of approximately 10% among the total number of bronchoscopies. Therefore, it can be deduced that the disease has a relatively high prevalence in the local population (especially among the elderly), which may

be related to the environmental conditions and lifestyle habits of residents in this region. Further studies on the prevention and treatment of BAF will be of significant value for clinical practice.

As reported in the literature, BAF may be classified as flat BAF, deep-seated retracted BAF, and protruding BAF. In addition to black lesions, bronchial swelling with infiltration, erythema, and thickening that may cause obliteration of bronchi may be observed[6]. The bronchoscopy results of the participants in this study revealed that participants with flat BAF (Fig. 1A) exhibited an unobstructed lumen with normal morphology; absence of evident mucosal hyperemia, edema, and thickening; and a sharp-appearing bronchial carina. In participants with deep-seated retracted BAF (Fig. 1B), we observed evident fibrous tissue proliferation, slight distortion of the lumen, stenosis of the affected bronchi (commonly occurring as external compression-type stenosis), slight hyperemia in the mucosa, and a sharp-appearing bronchial carina. Additionally, difficulties were encountered during the biopsy procedures of these participants. Bronchoscopies of participants with black mucosal protruding BAF (Fig. 1C) revealed severe distortion of the lumen; evident lumen stenosis often accompanied by bronchial obliteration; evident mucosal hyperemia, edema, and thickening; a broadened and deformed bronchial carina with occasional mucosal ulceration or undesirable deposits; and high bleeding tendency upon contact with the bronchoscope. Significant bleeding post-biopsy bleeding was observed (four participants experienced bleeding during bronchial brushing), and bleeding control was relatively difficult, although effective control was achieved after subsequent treatment. Among the 113 participants with BAF, 31 (27.4%) had flat BAF, 38 (33.6%) had deep-seated retracted BAF, and 44 (38.9%) had black mucosal protruding BAF. Based on the bronchoscopy features described herein, we have deduced that airway fibrosis is not the sole pathological characteristic of BAF. It is possible that angiogenesis is involved in the airway remodeling occurring in participants with BAF, thereby leading to a high tendency toward airway wall bleeding. Therefore, further investigation of the structural characteristics of the airway wall in BAF will be of significant clinical value.

The manifestations described above are merely macroscopic features observed under the bronchoscope. Currently, in-depth studies on the airway wall structures of participants with BAF remain scarce. Mirsadraee and Farshchi[13] performed EBUS on a participant with BAF and observed a scattered, nodular, hyperechoic pattern in the subepithelial area of the bronchus or lymph node adjacent to the bronchial mucosa. However, the authors could only achieve a preliminary understanding of the structural features of large airways due to the limitations of the medical equipment. In recent years, the clinical application of mini-probes in EBUS has provided favorable conditions for the assessment of distal small airways[14]. To determine the structural characteristics of small airways in BAF, we performed EBUS in participants with BAF and observed the presence of severe calcification and mucosal remodeling around the airways. Subsequently, ImageJ 18.0 was used to magnify the airway images of the various BAF subgroups for the measurement of airway wall indicators. As shown in Table 1 and Fig. 5, the maximum wall thicknesses of the deep-seated retracted BAF and black mucosal protruding BAF groups were significantly higher compared with that of the flat BAF group; the same was observed for the maximum submucosal thickness. Compared with the proportion of submucosal area ($64.8 \pm 9.1\%$) in the flat BAF group, the proportion ($30.4 \pm 8.8\%$) in the deep-seated retracted BAF group was significantly lower, but the

proportion ($58.6 \pm 11.7\%$) in the black mucosal protruding BAF group did not differ significantly from that of the flat BAF group. It can be deduced that different airway remodeling features may exist among different BAF subtypes, but a definite conclusion cannot be made due to the small sample size of this study. Therefore, the acquisition and analysis of ultrasound images and pathological examinations of participants with different types of BAF on a larger scale may provide conclusive evidence of airway structural changes associated with the disease.

In conclusion, different types of BAF exhibit different features under the bronchoscope, and differences have also been observed in airway walls upon further examination using EBUS. Therefore, differences in airway remodeling among the various BAF subtypes may lead to the manifestation of different clinical symptoms. Further study is required to elucidate the mechanisms by which airway remodeling in BAF causes different clinical symptoms. An adequate understanding of the airway remodeling characteristics and regulatory pathways of BAF may provide new clues for treatment of the disease.

Declarations

Authorship statement: Literature search: Xiaoyan Cai; Data collection: Qingshong Zeng and Li Zou; Study design: Zuoli Du; Data analysis: Xiaofeng Lu; Manuscript preparation: Xiaofeng Lu and Daishun Liu; Manuscript review: Guoqi Zhou

Disclosure statement: All authors have no conflicts of interest to declare.

Acknowledgments: This work was supported by grants from Zunyi City Science and Technology Plan (Zunshi Keheshe Zi [2018] 250), Honghuagang District Science and Technology Plan (Zunhong Keheshe Zi [2020] 12), and People's Hospital of Honghuagang District, Zunyi City, Talent Base Construction Project Plan.

Funding: This work was supported by grants from Zunyi City Science and Technology Plan (Zunshi Keheshe Zi [2018] 250), Honghuagang District Science and Technology Plan (Zunhong Keheshe Zi [2020] 12), and People's Hospital of Honghuagang District, Zunyi City, Talent Base Construction Project Plan [2020] 5.

Conflicts of interest/Competing interests: None to declare

Availability of data and material: The datasets used or analysed during the current study are available from the corresponding author on reasonable request.

Code availability: Not applicable

Authors' contributions: Literature search: Xiaoyan Cai; Data collection: Qingshong Zeng and Li Zou; Study design: Zuoli Du; Data analysis: Xiaofeng Lu; Manuscript preparation: Xiaofeng Lu and Daishun Liu; Manuscript review: Guoqi Zhou.

Ethics approval: This study was approved by the ethics committee of the People's Hospital of Honghuagang District.

Consent to participate: Due to the retrospective nature of the study, the requirement for informed consent was waived.

Consent for publication: Not applicable.

References

1. Shah A, Kunal S, Gothi R. Bronchial anthracofibrosis: the spectrum of radiological appearances. *Indian J Radiol Imaging*. 2018;28(3):33.
2. Sigari N, Mohammadi S. (2009) Anthracosis and anthracofibrosis. *Saudi Med J*. 2009;30:1063–1066.
3. Kim HY, Im JG, Goo JM, et al. Song JW. Bronchial anthracofibrosis (inflammatory bronchial stenosis with anthracotic pigmentation): CT findings. *AJR Am J Roentgenol*. 2000;174:523–7.
4. Mirsadraee M, Farshchi H. Endobronchial ultrasound in anthracosis. *J Bronchology Interv Pulmonol*. 2010;17:188–9.
5. Kim YJ, Jung CY, Shin HW, et al. (2009) Biomass smoke induced bronchial anthracofibrosis: presenting features and clinical course. *Respir Med*. 2009;103(5):757–765.
6. Amoli K. Anthracotic airways disease: report of 102 cases. *Tanaffos*. 2009;8:14–22.
7. Chung MP, Lee KS, Han J, et al. Bronchial stenosis due to anthracofibrosis. *Chest*. 1998;113:344–50.
8. Mireles-Cabodevila E, Karnak D, Shah SS, et al. Anthracostenosis *J Bronchol*. 2006;13:153–5.
9. Najafizadeh K, Zahirifard S, Mohammadi F, et al. Bronchial anthracofibrosis or anthracotic bronchitis. *Tanaffos*. 2003;2:7–11.
10. Wynn GJ, Turkington PM, O'Driscoll BR. Anthracofibrosis, bronchial stenosis with overlying anthracotic mucosa: possibly a new occupational lung disorder: a series of seven cases From one UK hospital. *Chest*. 2008;134:1069–73.
11. Hwang J, Puttagunta L, Green F, et al. Bronchial anthracofibrosis and tuberculosis in immigrants to Canada from the Indian subcontinent. *Int J Tuberc Lung Dis*. 2010;14:231–7.
12. An Yulin G, Jun Z, Mingqiang, et al. Clinical features of anthracosis and bronchial anthracofibrosis. *Chin J Respir Crit Care Med*. 2019;6:554–9.
13. Mirsadraee M, Farshchi H. Endobronchial ultrasound in anthracosis. *J Bronchology Interv Pulmonol*. 2010;17:188–9.
14. Gorska K, Korczynski P, Mierzejewski M, et al. Comparison of Endobronchial Ultrasound and High Resolution Computed Tomography as Tools for Airway Wall Imaging in Asthma and Chronic Obstructive Pulmonary Disease. *Respir Med*. 2016;117:131–8.

Tables

Table 1. Measurement values of endobronchial ultrasound images from various bronchial anthracofibrosis subgroups (mean±SD)

	Flat bronchial anthracofibrosis	Deep-seated retracted bronchial anthracofibrosis	Black mucosal protrusion bronchial anthracofibrosis	<i>F</i>	<i>P</i>
N	31 (27.4%)	38 (33.6%)	44 (38.9%)		
Maximum wall thickness (mm)	12.5±5.0	17.3±5.7	19.3±5.4	14.946	0.000
Maximum submucosal thickness (mm)	6.6±3.5	9.8±3.0	14.5±5.0	36.819	0.000
Proportion of submucosal area (%)	64.8±9.1	30.4±8.8	58.6±11.7	120.031	0.000
Proportion of bony tissue area (%)	33.3±9.3	65.2±8.7	34.9±12.1	113.473	0.000

Figures

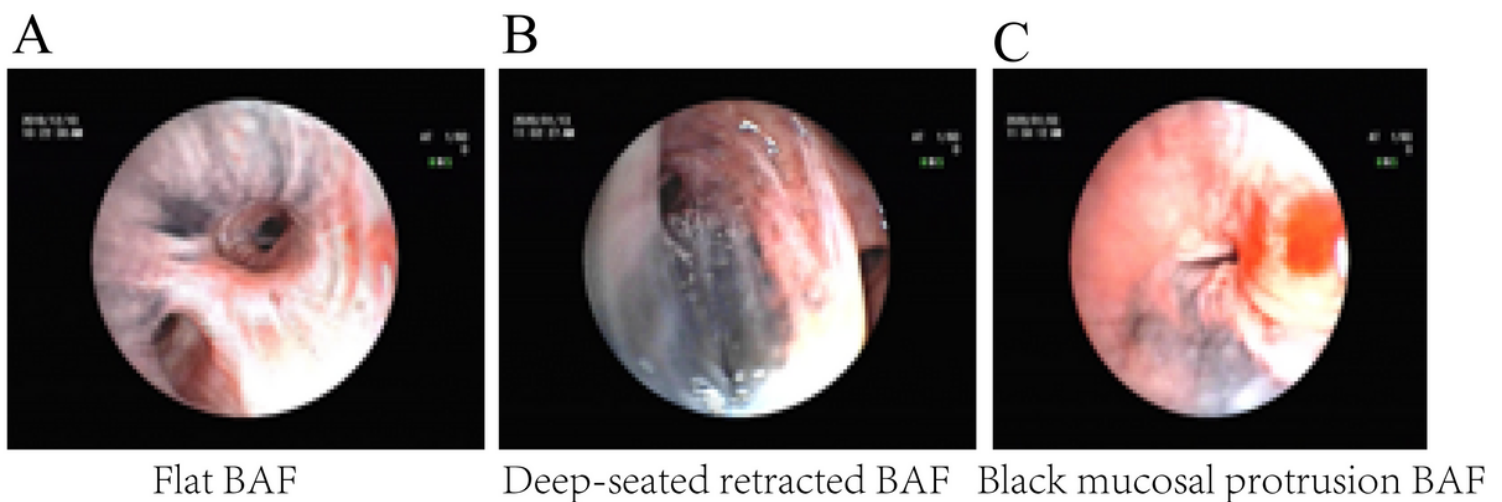


Figure 1

Bronchoscopy features of participants with different types of bronchial anthracofibrosis (A) Unobstructed lumen with normal morphology; absence of evident mucosal hyperemia, edema, and thickening; and a sharp-appearing bronchial carina. (B) Evident fibrous tissue proliferation, slight distortion of the lumen, stenosis of the affected bronchi (commonly occurring as external compression-type stenosis), slight

hyperemia in the mucosa, and a sharp-appearing bronchial carina. (C) Severe distortion of the lumen; evident lumen stenosis often accompanied by bronchial obliteration; evident mucosal hyperemia, edema, and thickening; a broadened and deformed bronchial carina with occasional mucosal ulceration or undesirable deposits; and high bleeding tendency upon contact with the bronchoscope

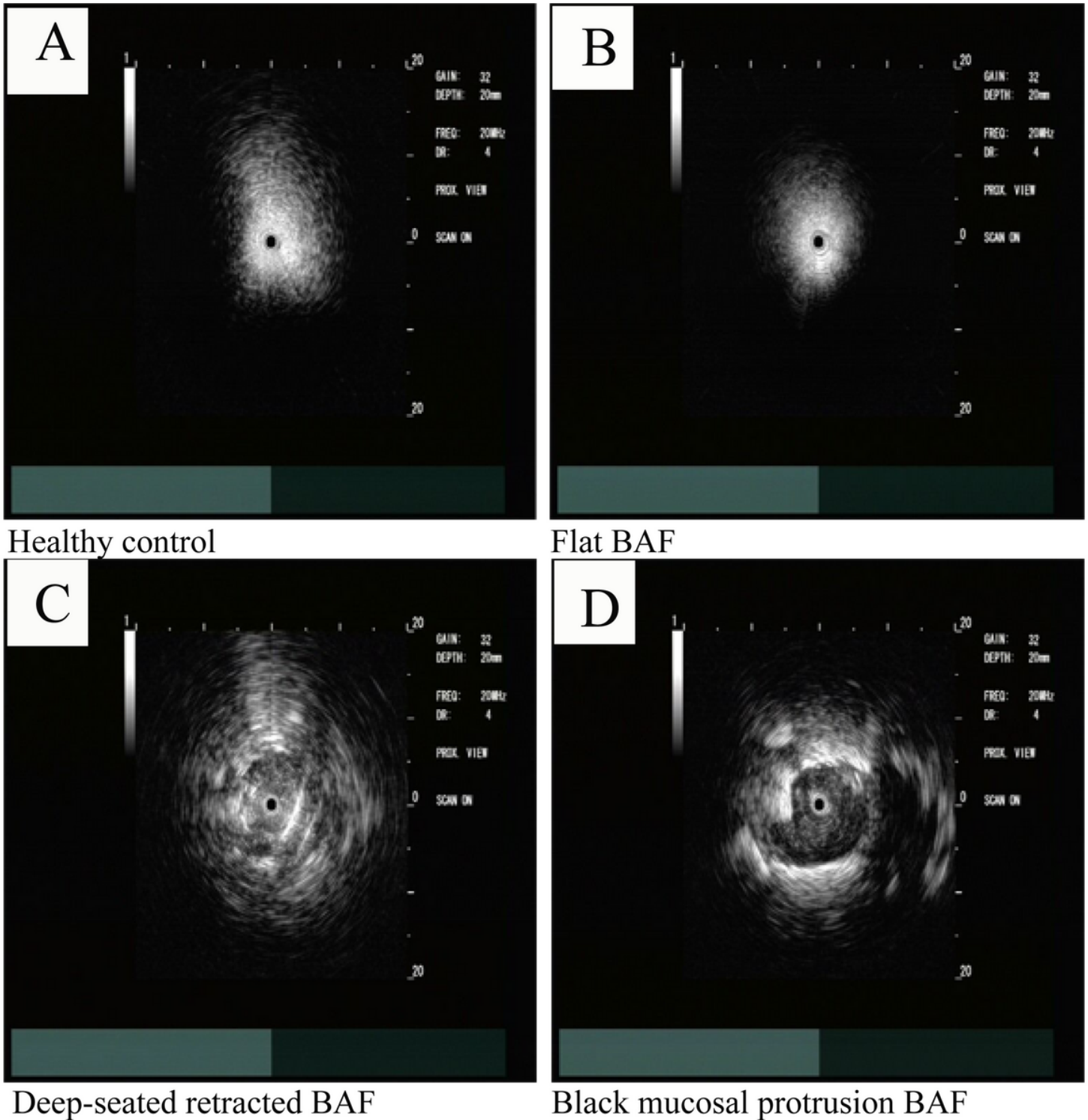


Figure 2

Ultrasound manifestations of lung tissue from participants with different types of bronchial anthracofibrosis (A) Uniform aeration patterns in the peripheral lung tissue. (B) Nonuniform aeration

patterns in the lung tissue. (C) Disordered lung tissue signals with scattered calcification patterns. (D) Soft tissue patterns in the lung tissue

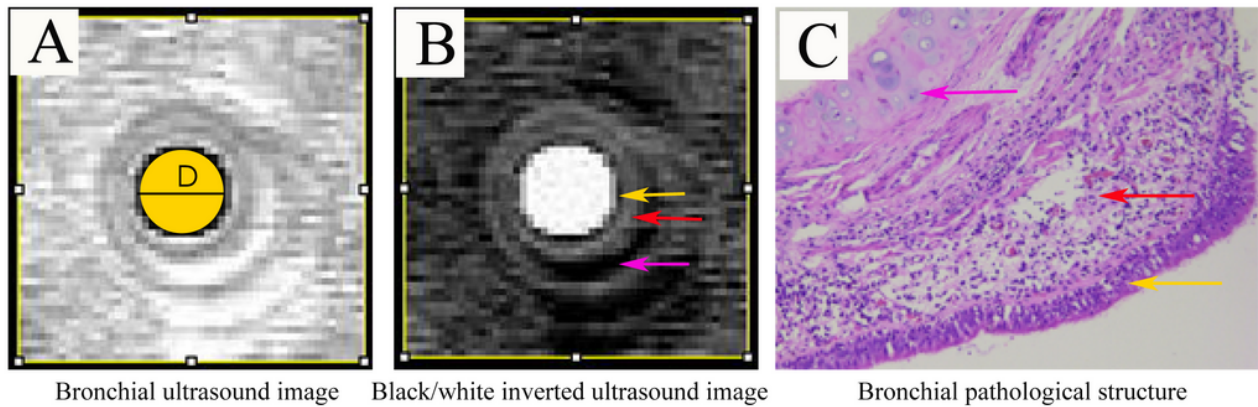


Figure 3

Bronchial ultrasound images and histopathology of bronchial tissue specimen from a participant with bronchial anthracofibrosis (BAF) (A) Magnified ultrasound image of a healthy airway with BAF. (B) Black/white inverted image of (A). (C) Histopathology of airway mucosal biopsy specimen (100× magnification). In Figure 3B and C, yellow arrows indicate the mucosa, red arrows indicate the submucosal tissue layers (including the basal lamina and smooth muscle layer), and pink arrows indicate the soft tissue. Acoustic shadows were present in the ultrasound images

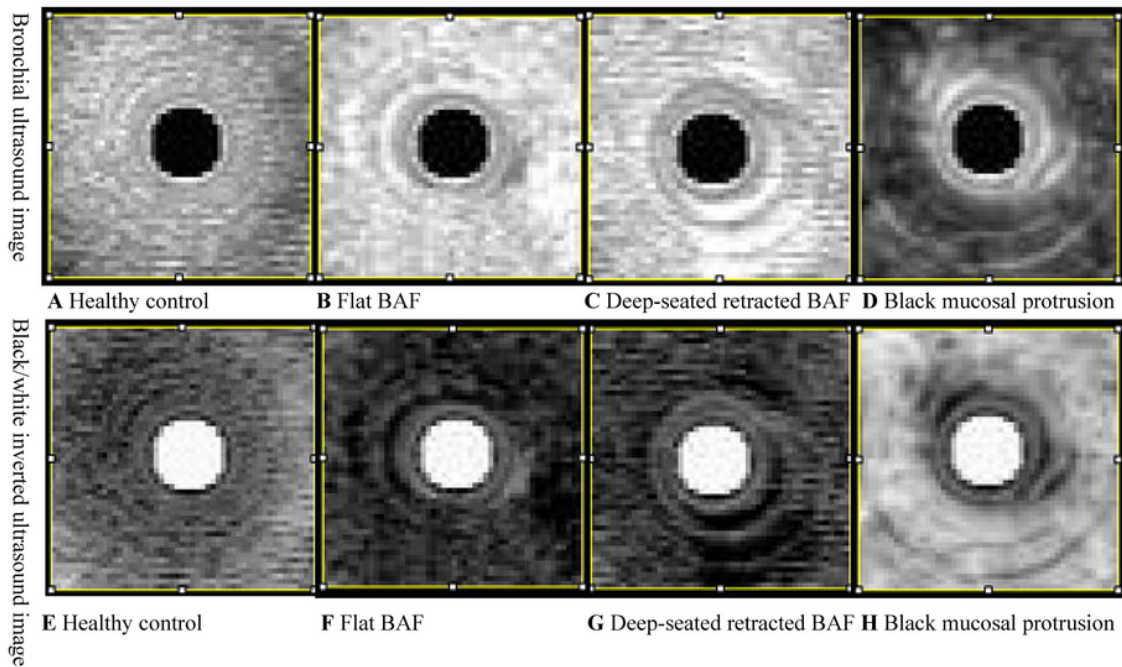


Figure 4

Bronchial ultrasound images of healthy control participants and participants with various types of bronchial anthracofibrosis

Healthy control group: a regular circular distribution of the airway wall, occasional shadows on the cartilage rings, uniform mucosa, and uniformly dense submucosal tissue; flat bronchial anthracofibrosis (BAF): decreased mucosal area compared with the healthy control group and uneven thickening of submucosal tissue; deep-seated retracted BAF: decreased mucosal area compared with the healthy control group, significant thickening of the cartilage layer, and uneven calcification on the airway wall; black mucosal protruding BAF: decreased mucosal area, uneven thickening of submucosal tissue, and a disorderly arrangement of cartilage tissue

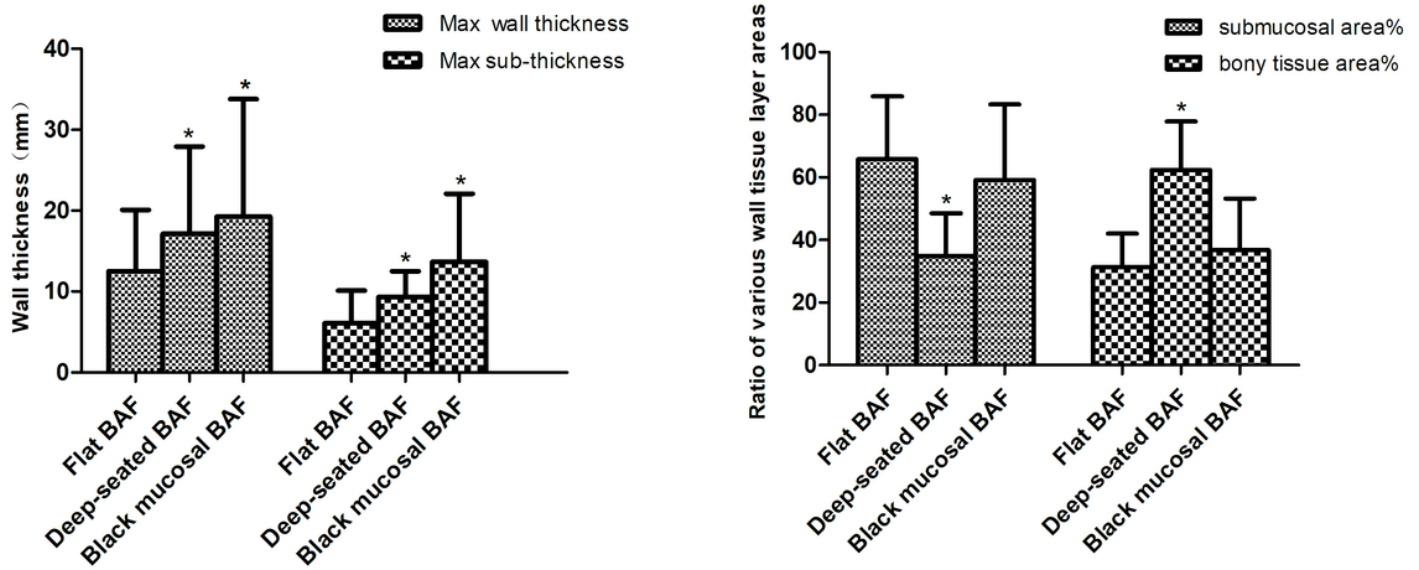


Figure 5

Comparison of the endobronchial ultrasound image measurement values in each subgroup of bronchial anthracofibrosis. By using ImageJ 18.0 to magnify the airways of each bronchial anthracofibrosis (BAF) subgroup, we measured the various indicators of the tube wall for statistical analysis. With respect to the maximum wall thickness, the deep-seated retracted BAF and the black mucosal protrusion BAF subgroups had significantly greater thickness compared with the flat BAF subgroup, and the difference was statistically significant ($P < 0.05$), while the deep-seated retracted BAF and the deep-seated retracted BAF subgroups showed no statistically significant difference ($P = 0.090$). As for the maximum submucosal thickness, the differences between the three groups were statistically significant ($P < 0.05$). The deep-seated retracted BAF group had a significantly higher proportion of bony tissue area than the flat BAF and the black mucosal protrusion BAF subgroups ($P < 0.05$), while the black mucosal protrusion BAF subgroup was not statistically significantly different compared with flat BAF subgroup ($P = 0.508$). With respect to the proportion of submucosal area, the differences between the three groups were statistically significant ($P < 0.05$).